Available online at www.sciencedirect.com
SCIENCE DIRECT®
International Journal of Thermal Sciences 45 (2006) 116–123
International Journal of Thermal Sciences
www.elsevier.com/locate/ijts

Local variation of frost layer thickness and morphology

Kaiyang Qu [a,*], Satoru Komori [a], Yi Jiang [b]

[a] *Department of Mechanical Engineering, Kyoto University, Kyoto 606-8501, Japan*
[b] *Department of Building Science, School of Architecture, Tsinghua University, Beijing 100084, China*

Received 8 September 2004; received in revised form 7 May 2005; accepted 26 May 2005

Available online 28 June 2005

Abstract

Frosting is an important phenomenon encountered in the cryogenic industries in connection with gas coolers, refrigerators, heat pumps, etc. It may adversely affect the performances of those devices. This paper experimentally studied the local frost formation process on a cold surface with natural airflows or forced airflows over it. The frost layer thickness was found to increase stepwise during the frost formation process. This increase pattern was ever indicated only by one literature. The literature attributed the pattern to the melting of frost crystals at the frost surface. However, present observation of the morphology of the frost layer surface suggested that the growth of water drops or ice particles at the initial period caused the first slowly increasing of the frost layer thickness; the following growth of acerose-shaped ice crystals caused the rapidly increasing of the frost layer thickness; thereafter, the column-shaped ice crystals on the surface grew in its length and radius alternatively, which caused the frost layer thickness increasing rapidly and slowly alternatively.

Keywords: Frost layer thickness; Stepwise increase; Morphology; Cold surface; Air flow

1. Introduction

When a cold surface with temperature below 0 °C is exposed to humid air, frost may deposit on the surface. This phenomenon is frequently encountered in the cryogenic industries in connection with gas coolers, refrigerators, heat pumps, etc. Frost deposition is usually undesirable. It may adversely affect the performance of devices due to the blocking of the air passages and the increase of the thermal resistance between air and the cold surface. Numerous studies have been conducted to study the frost formation process with intention to seek for countermeasures against frost formation.

Frost formation process on the cold surface was described as follows. Water vapor condenses on the cold surface in the form of supercooled liquid water droplets at first. The water droplets then grow and combine to form bigger water drops. Those bigger water drops freeze sometime and produce ice particles on the cold surface, which is usually regarded as the beginning of the frost formation process. Feather, rod or needle-shaped crystals then grow from the top of the ice particles. Those crystals first grow in the direction perpendicular to the surface at about the same rate. This period is called "crystal growth period" by Hayashi [1] or "one-dimensional growth period" by Tokura [2]. In the succeeding period, the frost grows not only in the direction perpendicular to the surface but also in the direction parallel to the surface. By the generation of branches around the top of the crystals, the frost layer grows gradually into a meshed and more uniform one. Frost layer surface becomes nearly flat. This period is called "frost layer growth period" by Hayashi [1] or "three-dimensional growth period" by Tokura [2]. At last, the frost surface temperature reaches 0 °C due to the increase of the frost layer thermal resistance. Water deposits on the frost surface instead of ice. The resultant water soaks into the ice layer and freeze. This period is called "frost layer full growth period" by Hayashi [1].

* Corresponding author. Present postal address: Department of Building Science, School of Architecture, Tsinghua University, Beijing 100084, China. Tel.: +86 10 62799780; fax: +86 10 62770544.
E-mail addresses: qukaiyang@tsinghua.edu.cn (K. Qu), komori@mech.kyoto-u.ac.jp (S. Komori), jiangyi@tsinghua.edu.cn (Y. Jiang).

1290-0729/$ – see front matter
doi:10.1016/j.ijthermalsci.2005.05.004

Thickness and thermal conductivity are the most important parameters of the frost layer since the negative effects of the frost layer lie in its blocking the air passage and increasing the thermal resistance between air and the cold surface. Most researchers tacitly agreed that the thickness of the frost layer increased continuously with time while the growing speed decreased gradually. Their experimental results consistently showed that the frost growth increased with the increasing air humidity and decreasing cold surface temperature and air temperature, both for natural and forced airflows. Whereas, the effect of the airflow conditions on the frost growth was rather confused with regard to forced airflows. O'Neal [3] concluded from his experimental results that frost growth increased with the increasing Reynolds number when Reynolds number was less than 15900, while had no dependence on the Reynolds number when Reynolds number was higher than 15900. O'Neal's conclusion for Reynolds number less than 15900 was supported by the experimental results of Brian [4] (with Reynolds numbers of 5100 and 5790), Sahin [5] (with Reynolds numbers of 2400, 3700, and 4500), and Lee [6] (with Reynolds number of 2000 and 1000). O'Neal's conclusion for Reynolds number higher than 15900 was supported by the experimental results of Trammell [7] (with Reynolds numbers of 2.40e+5 and 1.65e+5 as calculated by present authors), Yamakawa et al. [8] (with Reynolds numbers of 17508 and 25561 as calculated by present authors). There were other conclusions differing from O'Neal conclusion. Biguria's [9] experimental results showed that the frost growth increased with the increasing Reynolds number for Reynolds numbers of 4.66e+4, 1.24e+5, and 2.16e+5 (calculated by present authors). Schneider's [10] experimental results showed that there was no dependence of frost growth on Reynolds number for Reynolds numbers of 4000, 8000, 16000, and 32000. Han [11] indicated that the frost growth depended on the position rather than on Reynolds number for Reynolds numbers of 2270 and 1600. His experimental results showed that, at the front part of the plate, the frost growth at Reynolds number 1600 is stronger than that at Reynolds number 2270; at the middle part, they are almost equal; whereas at the rear part, the former became weaker than the latter. Cheng [12] employed a microscopic image system to record the pattern and the thickness of the frost layer. A multiple-step ascending frost growth pattern was observed. He attributed the pattern to the melting of frost crystals at the frost surface.

Thermal conductivity of the frost layer was usually calculated with the measured heat flux through the layer, temperatures of the cold surface and the frost surface and the frost layer thickness. For the frost formed under forced airflows, Biguria [9] indicated that the thermal conductivity of the frost layer might stepwise increase or fluctuate during the frost formation process depending on the concrete conditions. He concluded that the frost thermal conductivity should increase with air velocity linearly and with cold surface temperature by $T_p^{1.3}$, while the increasing air humidity might decrease the frost thermal conductivity at lower cold surface temperatures and increase it at higher cold surface temperatures. Ostin [15] indicated that, before the quasi-stationary condition was reached, the frost thermal conductivity decreased with the increasing of the frost layer thickness, while after that, the thermal conductivity increased linearly on the thickness of the frost layer. Shin's [16] experimental results showed that the frost thermal conductivity decreased at the initial period and then increased during the frost formation process. For the frost formed under natural airflows, Kennedy [13] indicated the thermal conductivity of the frost layer increased slightly with the increasing ambient humidity, while strongly with time (or frost thickness). Tajima [14] concluded that the conductivity of the frost layer just increased with the increasing specific weight of frost layer during the frost formation process. Researchers used to correlate the thermal conductivity of the frost layer to its density. The results were still not satisfactory.

Although numerous studies have been conducted on the frost formation process, the conclusions are rather diverse. Present authors conducted further studies on the frost formation process. This paper reports the stepwise increase of the local frost layer thickness during the frost formation process and tries to explain the mechanism behind it. This increase pattern of the frost layer thickness was seldom realized by researchers. However, it may be essential to elucidate the mechanism of frost growth.

2. Experimental apparatus and procedures

The experimental apparatus is schematically shown in Fig. 1. The apparatus was placed in a large laboratory room. A heater and a humidifier were employed to adjust the room temperature and humidity. Since the room had great thermal inertia, manual adjustment of the humidifier and heater could control the humidity and temperature of the room at stable values. Air in the room was sucked into the channel by the fan mounted at the end of the channel. It flew through the convergent section, screens, entrance section, test section and divergent section and then exit. The cross sections of the entrance section and the test section are both 160×15 mm^2. The entrance section was 1600 mm long, which made the air flow fully developed before entering the test section. An aluminum plate with area of 20×80 mm^2 was inlaid inside the upper plate of the channel in the test section. For the aspect ratio of the cross section of the channel is as high as 12, the flow over the aluminum plate can be regarded as two-dimensional one. A stainless steel vessel was put on the aluminum plate. During the experimental process, liquid nitrogen was held in the vessel. Then, the aluminum plate was cooled and frost grew on its bottom surface. Thermal insulation was inserted between the vessel and the aluminum plate to adjust the aluminum plate bottom surface temperature. The bottom plate of the channel in the test section was removed when experiments for natural airflow were conducted.

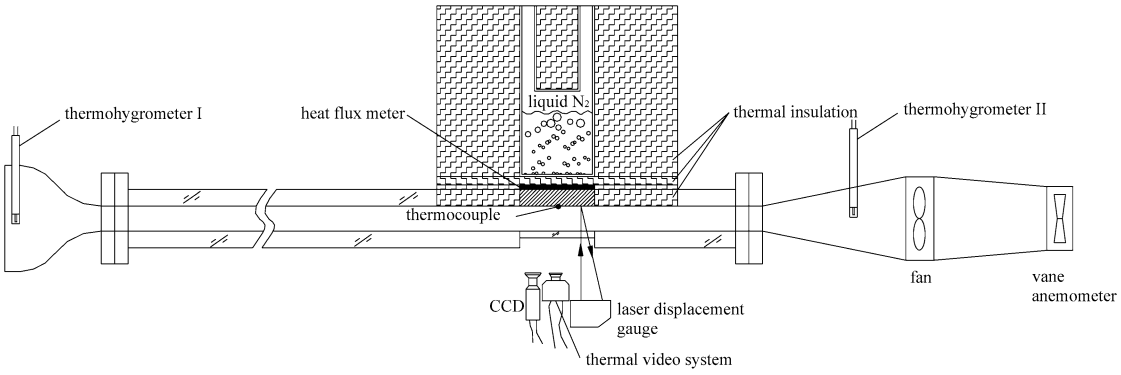

Fig. 1. Schematic of the experimental apparatus.

Table 1
Uncertainties of the measurement items

Measurement items	Instruments	Uncertainties
Air temperature entering the test section	Thermohygrometer I	±0.3 °C
Air relative humidity entering the test section	Thermohygrometer I	±3%
Air temperature leaving the test section	Thermohygrometer II	±0.3 °C
Air relative humidity leaving the test section	Thermohygrometer II	±3%
Air flow rate	Vane anemometer	±2%
Thickness of the frost layer	Laser displacement gauge	0.01 mm
Temperature of the frost layer surface	Thermal video system	±0.5 °C
Aluminum plate thermal conductivity	Thermal conductivity meter	±5%

Temperatures and relative humidities of air entering and leaving the test section were measured with the thermohygrometers placed at inlet and outlet of the test section. Air flow rate through the channel was measured with the vane anemometer attached to the channel end. Temperatures of the aluminum plate top and bottom surfaces were measured with the K type thermocouples attached to the surfaces. Heat flux through the aluminum plate could then be calculated with known plate conductivity. (The aluminum plate thermal conductivity was measured with a thermal conductivity meter in advance.) When the stable state was reached in the experiment, the heat flux through the aluminum plate could be considered to be equal to the heat flux through the frost layer. The frost layer surface temperature was measured with the thermal video system (TVS). The thickness of the frost layer was measured using the laser displacement gauge. Frost surface morphology was observed and recorded with the CCD camera. The uncertainties in the experimental measurements are shown in Table 1. The measurements of the frost layer thickness, the frost surface temperature, the cold surface temperature, and the heat flux were all made at the position 4 mm from the leading edge of the aluminum plate. The morphology of the frost surface was also taken around that position.

The thermal video system measured the surface temperature by detecting the radiation from the surface. Before the measurements could be conducted, the emissivity of the frost surface had to be determined. A special experiment was designed for that purpose. A temperature sensor was additionally set at the elevation of about 3 mm from the cold surface. When the surface of the growing frost layer reached the sensor, the temperature indicated by the sensor would abruptly decline. Immediately after that, the sensor indicated the temperature of the frost surface. The frost surface temperature was measured by the thermal video system simultaneously with an arbitrarily assigned frost surface emissivity. The emissivity was then modified based on the comparison of the two measured temperature values.

Methods to measure the thickness of the frost layer are divided into contact and non-contact ones. Simple contact methods based on touching of the frost surface by a fine thermocouple as a sensor were used by Hayashi [1] and Takura [2]. Non-contact methods were used by Cheng [12] and Besant [17]. Cheng [12] measured frost layer thickness by a microscopic image system. Besant [17] employed laser beam technique with the laser beam parallel to the frost surface to measure the average layer thickness. Laser beam technique was also employed in present study with the laser beam impinging the frost surface to measure the local thickness of the frost layer. The weak points of the contact method lied in the fact that a thermocouple might melt the frost around it and the sampling interval was rather long. In contrast, present laser beam technique affected little the frost surface and the sampling interval could be as short as 1 second. However, when the voids in the frost layer surface were too large, the incident laser might not be reflected effectively and the measurement failed. To weaken the adverse effect of the voids on the measurement, the laser beam impinged the frost surface with an angle less than 90° to the surface rather than perpendicularly to the surface.

3. Experimental results

Over 60 runs had been conducted for natural or forced airflows. Reynolds number ranged from 750 to 7400 for forced airflows. Since this paper focuses on the growing pattern of the frost, it will report only the results of several typical runs. The operational conditions for those runs are listed in Table 2.

3.1. Heat flux

When the stable state was reached in the experiment, the heat flux through the frost layer could be considered to be equal to the heat flux through the aluminum plate, which, q, is calculated by following equation:

$$q = \frac{(t_{\mathrm{pb}} - t_{\mathrm{pt}})\lambda_p}{\delta_p} \tag{1}$$

where, λ_p is the aluminum plate conductivity, δ_p is the aluminum plate thickness, t_{pt} is the aluminum plate top surface temperature, and t_{pb} is the aluminum plate bottom surface temperature.

Fig. 2 shows the variations of the heat flux through the frost layer during the frost formation process for cases 2 and 4. The Heat flux increased with time initially and then kept nearly constant. The latter periods of the runs could be regarded approximately as with constant heat flux.

3.2. Thickness of the frost layer

Fig. 3 shows the variations of the frost layer thickness as a function of time. The sampling interval was 1 second. In all the cases, including that under natural, for laminar and for turbulent airflows, the frost layer thickness increased stepwise during the frost formation process. In the initial period of the frost formation process, the frost layer thickness increased slowly. Following that, a steep increasing of the frost layer thickness was observed. Next, the increasing of the frost layer thickness became slow again. In such a way, the frost layer thickness increased rapidly and slowly alternatively through the whole frost formation process. The comparison between the cases shown in Fig. 3 also seems to suggest that increasing turbulence intensity and air humidity would increase the frequency of the cycle.

Table 2
Operational conditions of the runs

Case No.	*Re*	Temperature of air [°C]	Dew point of air [°C]	Heat flux[a] [W·m^2]
1	Natural airflow	25.3	17.0	750
2	1510	19.2	3.8	740
3	4980	19.5	1.4	1120
4	4980	18.1	1.1	1090
5	4980	18.8	11.0	1060

[a] The heat fluxes shown in this table indicate the heat fluxes in the latter periods of the frost formation process, when the heat fluxes kept approximately constant.

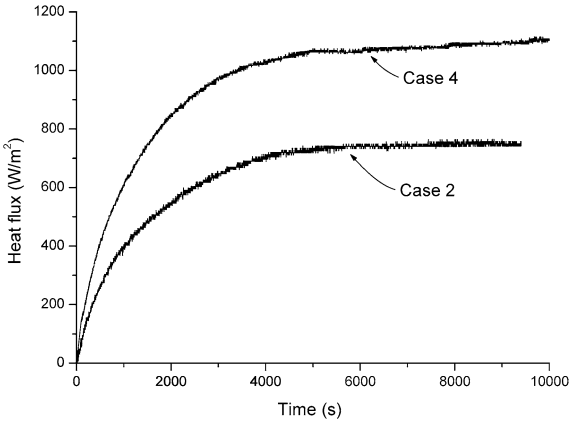

Fig. 2. Typical results showing the variations of the heat flux through the frost layer during the frost formation process.

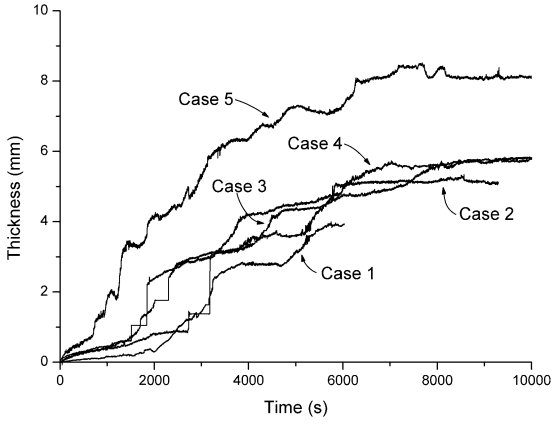

Fig. 3. Variations of the frost layer thickness during the frost formation process.

When acerose-typed ice crystals formed on the frost layer surface, the incident laser might not be reflected effectively by the frost surface and the displacement gauge might thus fail to work. In that situation, the displacement gauge yielded unvaried signals. In Fig. 3, the short, smooth and level sections of the curves for cases 2, 3, and 4 just indicate the failure of the displacement gauge. Since those sections are very short compared to the whole curve, they do not affect the conclusion that the frost layer thickness increased stepwise through the whole frost formation process.

3.3. Average thermal conductivity

The average thermal conductivity of the frost layer, λ_f, is calculated by following equation:

$$\lambda_f = \frac{q\delta_f}{(t_f - t_{\mathrm{pb}})} \tag{2}$$

where, q is the heat flux through the frost layer as calculated by Eq. (1), δ_f is the frost layer thickness, t_{pb} is the aluminum plate bottom surface temperature, and t_f is the frost layer surface temperature.

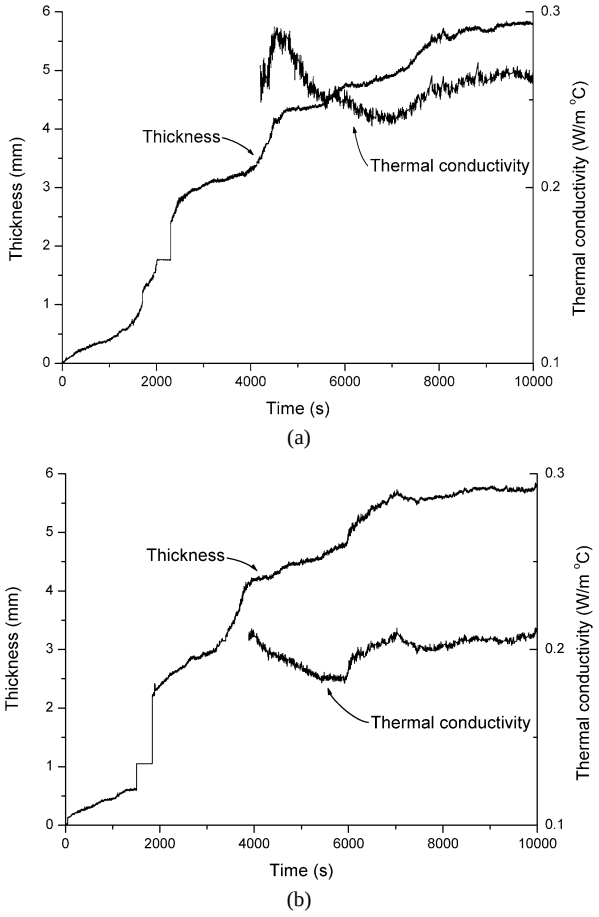

Fig. 4. Variations of the surface temperature and the thermal conductivity of the frost layer during the frost formation process, (a) for case 3 and (b) for case 4.

Fig. 4 shows the average thermal conductivity for cases 3 and 4 together with the variation of the thickness of the frost layer. Since the thermal video system measures the surface temperature by detecting the radiation from the surface, it fails to work properly when there were too big voids in the surface. In the present experiments, the surface temperature could be measured convincingly only in the latter periods of frost formation process. So, only in those periods was the average thermal conductivity measured validly. As indicated by Fig. 4, the thermal conductivity of the frost layer fluctuated with frost growth in the latter periods of frost formation process. The amplitude of the fluctuation was, however, unremarkable.

3.4. Morphology of the frost layer surface

A CCD camera was employed to observe the morphology of the frost layer surface with the intention to elucidate how the frost layer thickness increases in the stepwise pattern. Fig. 5 shows serially the images of the frost layer surface during the frost formation process of case 3. Fig. 6 shows the correspondence between the images and the frost layer thickness variation.

The morphology of the frost surface changed continually during the whole process. As the cold surface temperature decreased, water droplets formed on the surface. The water droplets grew and merged into bigger drops until freezing sometime, when ice particles appeared on the surface (see Fig. 5(a)). The ice particles are relatively far apart from each other initially. They grew gradually in all directions. Next, acerose-shaped ice crystals grew sporadically from the top of the ice particles (see Fig. 5(b)). They grew mainly in the normal direction of the surface. In this period, the thickness of the frost layer increased rapidly. The void portion occupied most area of the frost layer surface, which rendered the thermal video system and the displacement gauge to fail to work sometimes. These crystals then changed to grow mainly in the direction parallel to the cold surface and showed feather shape (see Fig. 5(c)). The void portion of the frost layer surface was rapidly filled by those ice crystals. Then, column-shaped or needle-shaped crystals began to appear on the surface. The column-shaped crystals on the surface grew initially mainly in its radius rather than in its length. As a result, the crystals perpendicular to the surface increased their cross section areas (as seen in the frames at the right-top corner of Fig. 5(d)–(f)). The crystals lying across the surface increased their width (as seen in the frames at the left-bottom corner of Fig. 5(d)–(f)). From Fig. 5(d)–(f), the frost layer thickness increased slowly. Then the crystals on the surface resume growing mainly in its length. The crystals in the frames of Fig. 5(g)–(i) could be seen to become longer and longer with the radius changing little. The thickness of the frost layer increased rapidly again in this period. From Fig. 5(j)–(l), the crystals on the surface grow again mainly in their radius and the thickness of the frost layer increased slowly. An example could be seen in the frames in the figures. From Fig. 5(m)–(o), the crystals on the surface changed again to grow mainly in their length and the thickness of the frost layer increased relatively rapidly. An example was shown in the frames in the figures. From Fig. 5(p)–(r), the crystals on the surface grow again mainly in their radius, as seen with the crystal in the frames in the figures. The frost layer thickness increased again relatively slowly.

The observation on the morphology of the frost layer surface suggested the following fact. The first slowly increasing period just corresponded to the growth of water drops or ice particles. The first rapidly increasing period just corresponded to the growth of acerose-shaped ice crystals. Thereafter, the column-shaped ice crystals on the surface grew in its length and radius alternatively and caused the frost layer thickness to increase rapidly and slowly alternatively.

4. Discussions

The stepwise increase of the frost layer thickness was ever indicated only by Cheng [12]. However, it can be found with other researcher's results when they are checked carefully. Fig. 7 shows the experimental results by Ostin [15],

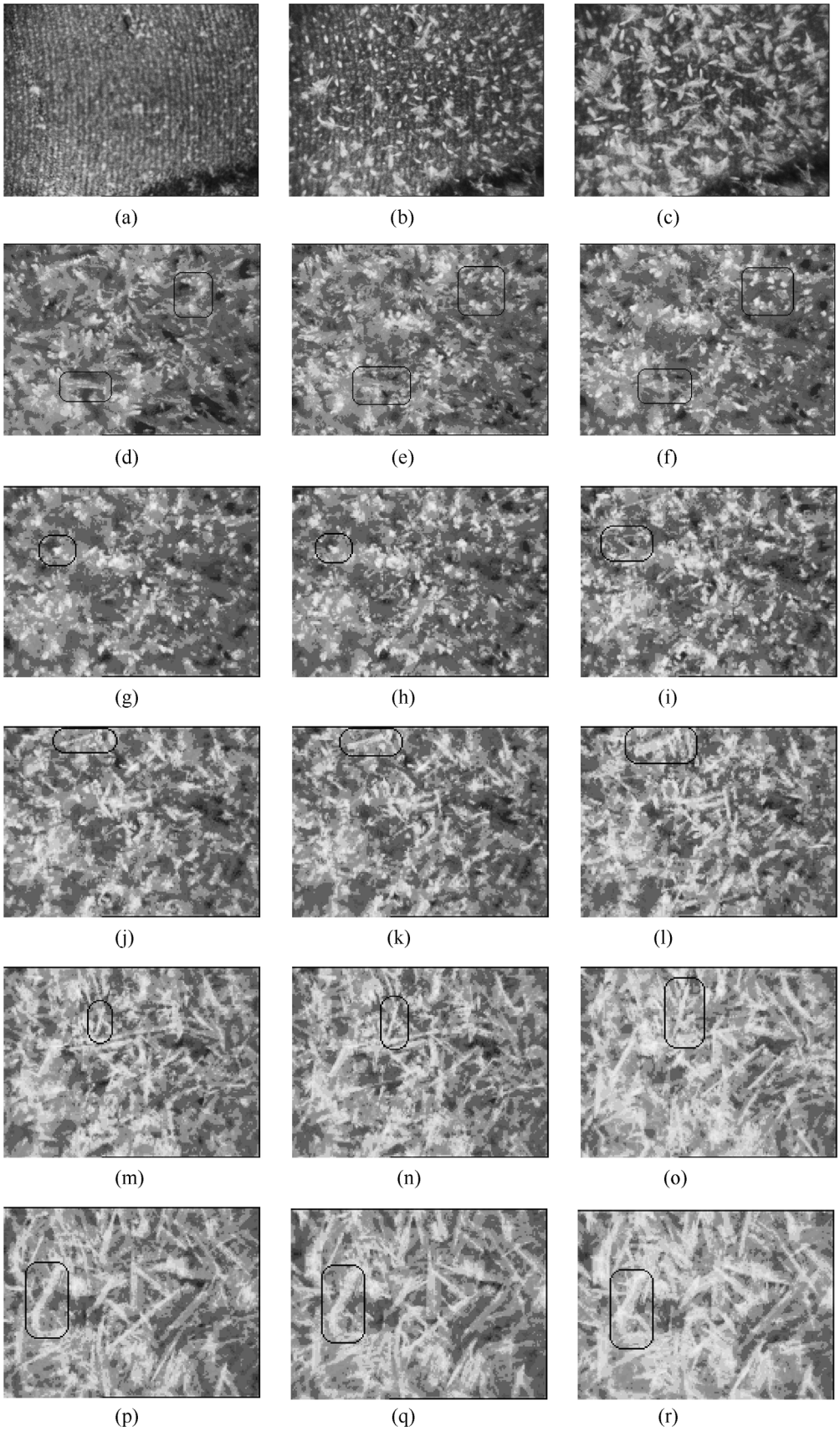

Fig. 5. Serial images of the frost layer surface during the frost formation process of case 3, viewed from above.

Lee [18], and Yonko (cited from [19] by Sami) for forced airflows and that by Tajima [14] for natural airflows. The data points obviously indicate the stepwise increase of the frost layer thickness both for natural and forced airflows. However, the researchers tried to fit the points with a smooth curve and hence smeared such kind of tendency. This oversight in the previous studies may be attributed to that the sampling time intervals were somewhat long (around 10 minutes or longer) and the confirmation of such kind of tendency became risky.

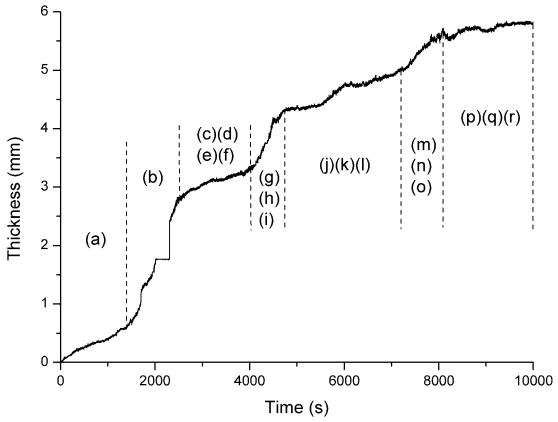

Fig. 6. Correspondence between the images shown in Fig. 5 and the variation of the frost layer thickness during the frost formation process of case 3.

Cheng [12] considered the stepwise increase of the frost layer thickness was caused by melting of frost crystals at the frost layer surface. However, no water was observed on the frost layer surface in present experiments while the frost layer thickness increased stepwise. Present observation on the morphology of the frost layer surface suggested the stepwise increase of the frost layer thickness was mainly caused by ice crystals on the surface growing in its length and radius alternatively.

The growth of ice crystals has been studied extensively with the background to study the snowing process. Generally, hexagonal prism shaped ice crystals tend to grow merely in its length or radius under certain ambient conditions and finally form long and thin or short and flat shapes [20], as seen in Fig. 8. That conclusion may explain present results quantitatively. In the frost formation process, the frost layer keeps varying in its height or thermal resistance. As a consequent, its surface conditions, including temperature of

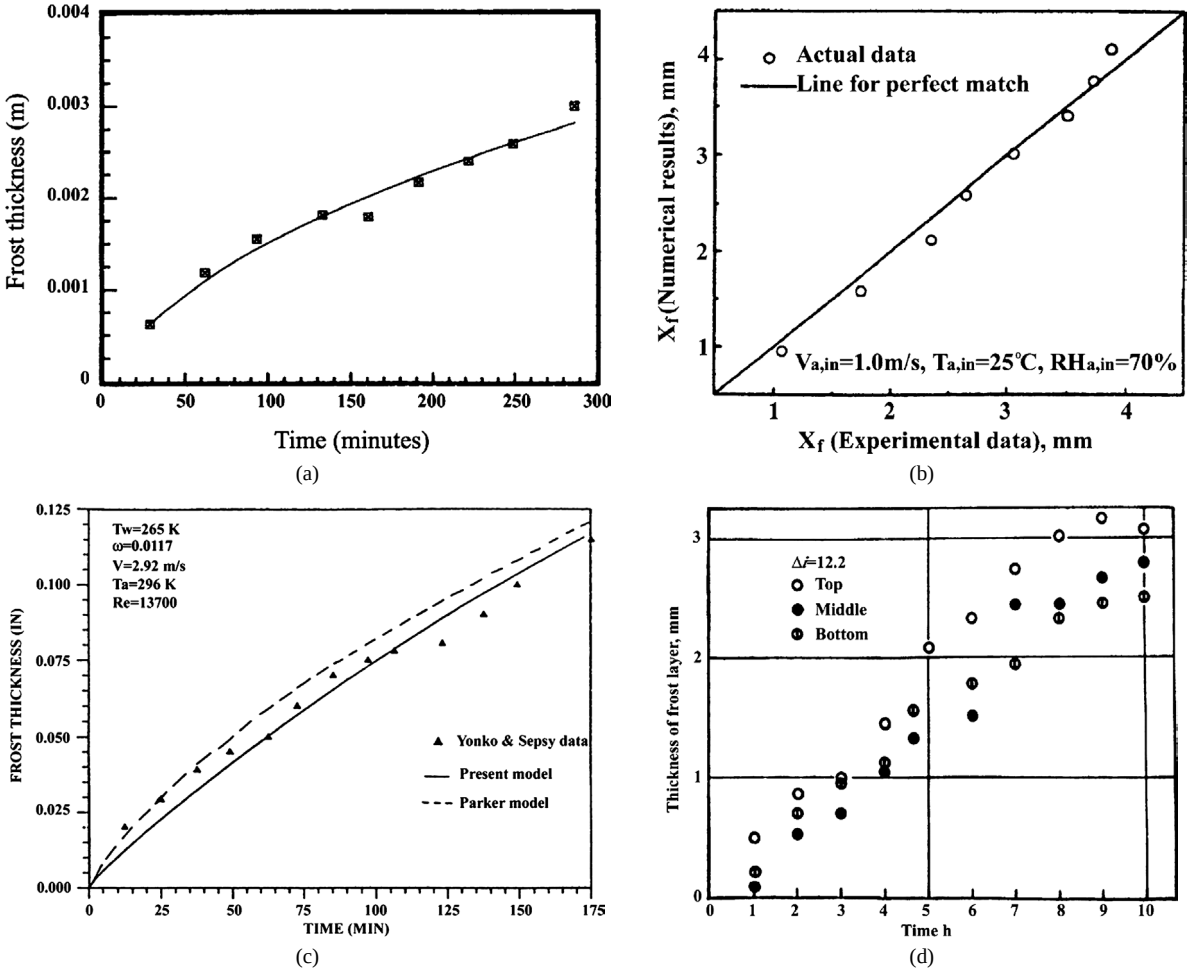

Fig. 7. Graphs cited from literatures showing the stepwise increase of the frost layer thickness during the frost formation process: (a) by Ostin [15]; (b) by Lee [18]; (c) by Sami [19]; (d) by Tajima [14].

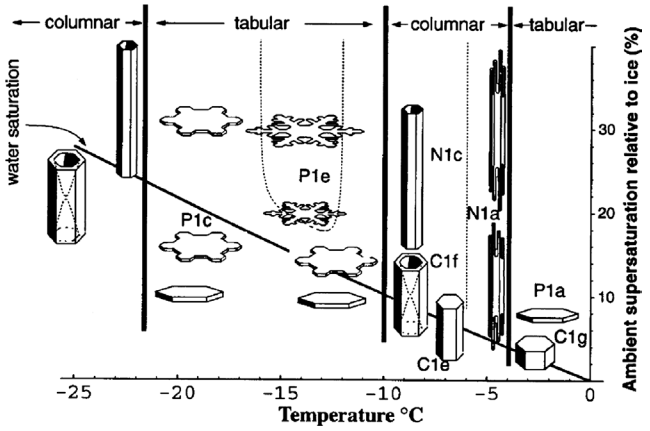

Fig. 8. Diagram of snow crystal growth habits after about 10 min growth at 1 atm at various ambient temperatures and supersaturations, duplicated from [20].

the surface and water vapor supersaturation around the surface keeps varying. According to Fig. 8, at critical points, the change of the frost layer surface conditions may cause ice crystals to change their growth habits. That is, the ice crystals may change from growing in its length to in its radius or vice versa at critical points, which would lead to the stepwise increase of the frost layer thickness as observed in present experiments.

5. Conclusions

This paper experimentally studied the local frost formation process on a cold surface with forced or natural airflows over it. Frost layer was found to increase stepwise during the whole frost formation process whatever for natural or for forced airflows. The average thermal conductivity of the frost layer could be measured only in the latter periods of the frost formation process. It fluctuated slightly corresponding to rapidly or slowly increasing periods of the frost layer thickness.

No water was observed on the frost layer surface in present experiments while the frost layer thickness increased stepwise. So, it was hard to attribute the stepwise increase pattern of the frost layer thickness to melting of the ice crystals on the frost layer, as done by Cheng [12]. Present observation of the morphology of the frost layer surface suggested that the first slowly increasing period just corresponded to the growth of water drops or ice particles; the first rapidly increasing period just corresponded to the growth of acerose-shaped ice crystals; thereafter, the column-shaped ice crystals on the surface grew in its length and radius alternatively, which led to the frost layer thickness increasing rapidly and slowly alternatively.

Acknowledgement

Kaiyang Qu would like to thank JSPS (Japan Society for the Promotion of Sciences) for supporting his stay at Kyoto University as an JSPS fellow.

References

[1] Y. Hayashi, A. Aoki, S. Adachi, K. Hori, Study of frost properties correlating with frost formation types, J. Heat Transfer 99 (1977) 239–245.
[2] I. Tokura, H. Saito, K. Kishinami, Study on properties and growth rate of frost layers on cold surfaces, J. Heat Transfer 105 (1983) 895–901.
[3] D.L. O'Neal, D.R. Tree, Measurement of frost growth and density in a parallel plate geometry, ASHRAE Trans. 90 (2) (1984) 278–289.
[4] P.L.T. Brian, R.C. Reid, Y.T. Shah, Frost deposition on cold surfaces, Indust. Engrg. Chem. Fund. 9 (1970) 375–380.
[5] A.Z. Sahin, An experimental study on the initiation and growth of frost formation on a horizontal plate, Experimental Heat Transfer 7 (1994) 101–119.
[6] Y.B. Lee, S.T. Ro, Frost formation on a vertical plate in simultaneously developing flow, Experimental Thermal Fluid Sci. 26 (2002) 939–945.
[7] G.J. Trammell, D.C. Little, E.M. Killgore, A study of frost formed on a flat plate held at sub-freezing temperatures, ASHRAE J. (July 1968) 42–47.
[8] N. Yamakawa, N. Takehashi, S. Ohtani, Forced convection heat and mass transfer under frost conditions, Heat Transfer Japan. Res. 1 (1972) 1–10.
[9] G. Biguria, L.A. Wenzel, Measurement and correlation of water frost thermal conductivity and density, I&EC Fund. 9 (1970) 129–137.
[10] H.W. Schneider, Equation of the growth rate of frost forming on cooled surfaces, Internat. J. Heat Mass Transfer 21 (1978) 1019–1024.
[11] H.D. Han, S.T. Ro, The characteristics of frost growth on parallel plates, in: K. Hutter, Y. Wang, H. Beer (Eds.), Advances in Cold-Region: Thermal Engineering and Sciences-Technological, Environmental and Climatological Impact, Proceedings of the 6th International Symposium, Springer, Berlin, 1999, pp. 22–25.
[12] C.H. Cheng, K.H. Wu, Observations of early-stage frost formation on a cold plate in atmospheric air flow, J. Heat Transfer 125 (2003) 95–102.
[13] L.A. Kennedy, J. Goodman, Free convection heat and mass transfer under conditions of frost deposition, Internat. J. Heat Mass Transfer 17 (1974) 477–484.
[14] O. Tajima, E. Naito, K. Nakashima, H. Yamamoto, Frost formation on air coolers (part 3, natural convection for cooled vertical plate), Heat Transfer Japan. Res. 3 (1974) 55–66.
[15] R. Ostin, S. Andersson, Frost growth parameters in a forced air stream, Internat. J. Heat Mass Transfer 34 (1990) 1009–1017.
[16] J. Shin, A.V. Tikhonov, C. Kim, Experimental study on frost structure on surfaces with different hydrophilicity: Density and thermal conductivity, J. Heat Transfer 125 (2003) 84–94.
[17] R.W. Besant, K.S. Reakallah, Y. Mao, J. Falk, Measurements of frost thickness using a laser beam and light meter, ASHRAE Trans. 96 (1990) 519–522.
[18] K.S. Lee, W.S. Kim, T.H. Lee, A one-dimensional model for frost formation on a cold flat surface, Internat. J. Heat Mass Transfer 40 (1997) 4359–4365.
[19] S.M. Sami, T. Duong, Mass and heat transfer during frost growth, ASHRAE Trans. 95 (2) (1989) 267–290.
[20] J. Nelson, Growth mechanism to explain the primary and secondary habits of snow crystals, Philos. Magazine A 81 (2001) 2337–2373.